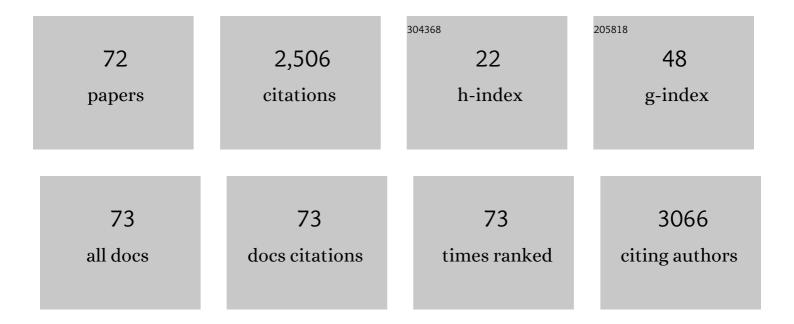
## List of Publications by Year in descending order

Source: https://exaly.com/author-pdf/8863936/publications.pdf

Version: 2024-02-01



Lii Lii

#	Article	IF	CITATIONS
1	Optimized tellurite glasses containing CsPbBr3-quantum dots for white-light emitting diodes. Journal of Non-Crystalline Solids, 2022, 581, 121429.	1.5	14
2	Significant Fluorescence Enhancement through Rapid Laser Annealing and Nonthermal Coupling Optical Temperature Sensing of Er-Doped Yttria Nanocrystals. Journal of Physical Chemistry C, 2022, 126, 3830-3838.	1.5	7
3	Dual-excitation regulated Tm3+ upconverting luminescence towards novel encrypted information transmission. Optical Materials, 2022, 127, 112258.	1.7	1
4	Suppression of inner energy dissipation in Yb-doped NaErF4 upconversion nanocrystals through an energy cycling strategy. Journal of Rare Earths, 2022, , .	2.5	0
5	800 nm laser induced white light upconversion of Nd/Yb/Pr triply doped NaYF4 through a dual-sensitization strategy. Materials Research Bulletin, 2021, 133, 111027.	2.7	9
6	Photothermal control of whispering gallery mode lasing in polymer-coated silica microcavity using high-efficiency nanoheater. Journal of Materials Science, 2021, 56, 570-580.	1.7	6
7	A new role of Yb <sup>3+</sup> —an energy reservoir for lanthanide upconversion luminescence. Nanoscale, 2021, 13, 9978-9988.	2.8	9
8	Compact all-fiber thermo-optic modulator based on a Michelson interferometer coated with NaNdF <sub>4</sub> nanoparticles. Optics Express, 2021, 29, 6854.	1.7	5
9	Color tuning in a compact core-shell nanocrystal based on intense and high-purity green and red photon upconversion. Optics Letters, 2021, 46, 900.	1.7	5
10	Highly stable CsPbBr <sub>3</sub> perovskite quantum dot-doped tellurite glass nanocomposite scintillator. Optics Letters, 2021, 46, 3448.	1.7	21
11	Precisely Designed Mesoscopic Titania for High-Volumetric-Density Pseudocapacitance. Journal of the American Chemical Society, 2021, 143, 14097-14105.	6.6	30
12	Optical fiber sensor based on upconversion nanoparticles for internal temperature monitoring of Li-ion batteries. Journal of Materials Chemistry C, 2021, 9, 14757-14765.	2.7	20
13	Mechanisms of Upconversion Luminescence of Er3+-Doped NaYF4 via 980 and 1530 nm Excitation. Nanomaterials, 2021, 11, 2767.	1.9	7
14	Effects of inert shell on the upconversion intensity and color of Na(Er/Yb)F4 nanocrystals. AIP Advances, 2021, 11, 105312.	0.6	1
15	Tm <sup>3+</sup> heavily doped NIR-III bioprobe with 1 µm Stokes shift towards deep-tissue applications. Optics Express, 2021, 29, 42674.	1.7	3
16	Temperature-Independent Lifetime and Thermometer Operated in a Biological Window of Upconverting NaErF4 Nanocrystals. Nanomaterials, 2020, 10, 24.	1.9	25
17	Functionalised liquid crystal microfibers for hydrogen peroxide and catalase detection using whispering gallery mode. Liquid Crystals, 2020, 47, 1708-1717.	0.9	9
18	Solvent-Assisted Self-Assembly of a Metal–Organic Framework Based Biocatalyst for Cascade Reaction Driven Photodynamic Therapy. Journal of the American Chemical Society, 2020, 142, 6822-6832.	6.6	201

#	Article	IF	CITATIONS
19	Sub-10 nm NaNdF <sub>4</sub> Nanoparticles as Near-Infrared Photothermal Probes with Self-Temperature Feedback. ACS Applied Nano Materials, 2020, 3, 2517-2526.	2.4	29
20	Size and charge dual-transformable mesoporous nanoassemblies for enhanced drug delivery and tumor penetration. Chemical Science, 2020, 11, 2819-2827.	3.7	66
21	Intense and color-tunable upconversion through 980 and 1530Ânm excitations. Journal of Luminescence, 2020, 224, 117306.	1.5	12
22	Self-monitored biological nanoheaters operating in the first biological window based on single-band red upconversion nanoparticles fabricated through architectural design. Journal of Alloys and Compounds, 2020, 842, 155602.	2.8	11
23	Nanoheater-tuned whispering gallery mode lasing in liquid-filled hollow microcavities. Optics Letters, 2020, 45, 815.	1.7	7
24	Correlation between ultrabroadband nearâ€infrared emission and Yb <sup>3+</sup> /Ni <sup>2+</sup> dopants distribution in highly transparent germanate glassâ€ceramics containing zinc gallogermanate nanospinels. Journal of the American Ceramic Society, 2019, 102, 1619-1627.	1.9	4
25	Upconversion enhancement through a facile, ultrafast, and low-threshold laser annealing strategy. Nanotechnology, 2019, 30, 435703.	1.3	8
26	Elemental Migration in Core/Shell Structured Lanthanide Doped Nanoparticles. Chemistry of Materials, 2019, 31, 5608-5615.	3.2	49
27	Facile preparation of upconversion microfibers for efficient luminescence and distributed temperature measurement. Journal of Materials Chemistry C, 2019, 7, 7984-7992.	2.7	18
28	Novel optical thermometer through upconversion emission of Ho3+ sensitized by Nd3+. Journal of Luminescence, 2019, 213, 40-45.	1.5	22
29	<i>In Vivo</i> High-resolution Ratiometric Fluorescence Imaging of Inflammation Using NIR-II Nanoprobes with 1550 nm Emission. Nano Letters, 2019, 19, 2418-2427.	4.5	202
30	Efficient nanoheater operated in a biological window for photo-hyperthermia therapy. Biomedical Optics Express, 2019, 10, 1935.	1.5	15
31	Highly efficient upconversion luminescence of Er heavily doped nanocrystals through 1530  nm excitation. Optics Letters, 2019, 44, 711.	1.7	19
32	Ultrabright single-band red upconversion luminescence in highly transparent fluorosilicate glass ceramics containing KMnF <sub>3</sub> perovskite nanocrystals. Optics Letters, 2019, 44, 2959.	1.7	12
33	Efficient green upconversion luminescence in highly crystallized ultratransparent nano-glass ceramics containing isotropic KY <sub>3</sub> F <sub>10</sub> nanocrystals. Optics Letters, 2019, 44, 4674.	1.7	18
34	Preparation and upconversion properties of rare earth doped core-shell Y(OH)3 and β-NaYF4 hybrid nanorods. Materials Research Bulletin, 2018, 101, 61-66.	2.7	6
35	The distribution of rare earth ions in a γ-Ga <sub>2</sub> O <sub>3</sub> nanocrystal-silicate glass composite and its influence on the photoluminescence properties. Journal of Materials Chemistry C, 2018, 6, 2944-2950.	2.7	29
36	Near-infrared rechargeable "optical battery―implant for irradiation-free photodynamic therapy. Biomaterials, 2018, 163, 154-162.	5.7	83

#	Article	IF	CITATIONS
37	Er <sup>3+</sup> Sensitized 1530â€nm to 1180â€nm Second Nearâ€Infrared Window Upconversion Nanocrystals for Inâ€Vivo Biosensing. Angewandte Chemie - International Edition, 2018, 57, 7518-7522.	7.2	271
38	Supramolecularly Engineered NIRâ€I and Upconversion Nanoparticles In Vivo Assembly and Disassembly to Improve Bioimaging. Advanced Materials, 2018, 30, e1804982.	11.1	146
39	Upconversion thermometer through novel PMMA fiber containing nanocrystals. Optical Materials Express, 2018, 8, 2321.	1.6	13
40	Concentration dependent optical transition probabilities in ultra-small upconversion nanocrystals. Optics Express, 2018, 26, 23471.	1.7	18
41	Highly sensitive and accurate optical thermometer through Er doped tellurite glasses. Materials Research Bulletin, 2018, 105, 306-311.	2.7	31
42	Dispersing upconversion nanocrystals in PMMA microfiber: a novel methodology for temperature sensing. RSC Advances, 2018, 8, 19362-19368.	1.7	9
43	NIR-II nanoprobes in-vivo assembly to improve image-guided surgery for metastatic ovarian cancer. Nature Communications, 2018, 9, 2898.	5.8	343
44	Phase transformation and controllable size of γ-Al <sub>2</sub> O <sub>3</sub> nanocrystals through Li doping using sol–gel method. Phase Transitions, 2018, 91, 1129-1134.	0.6	3
45	Topological Engineering of Photoluminescence Properties of Bismuth―or Erbiumâ€Đoped Phosphosilicate Glass of Arbitrary P <sub>2</sub> O <sub>5</sub> to SiO <sub>2</sub> Ratio. Advanced Optical Materials, 2018, 6, 1800024.	3.6	19
46	Er <sup>3+</sup> Sensitized 1530â€nm to 1180â€nm Second Nearâ€Infrared Window Upconversion Nanocrystals for Inâ€Vivo Biosensing. Angewandte Chemie, 2018, 130, 7640-7644.	1.6	41
47	Enlarged memory margins for resistive switching devices based on polyurethane film due to embedded Ag nanoparticles. Solid-State Electronics, 2018, 147, 6-12.	0.8	6
48	Unipolar nonvolatile memory devices based on the composites of poly(9-vinylcarbazole) and zinc oxide nanoparticles. Journal of Materials Science: Materials in Electronics, 2017, 28, 11749-11754.	1.1	8
49	Orthogonal Multiplexed Luminescence Encoding with Nearâ€Infrared Rechargeable Upconverting Persistent Luminescence Composites. Advanced Optical Materials, 2017, 5, 1700680.	3.6	52
50	Atomic Mechanism of Interfacial-Controlled Quantum Efficiency and Charge Migration in InAs/GaSb Superlattice. ACS Applied Materials & Interfaces, 2017, 9, 26642-26647.	4.0	12
51	Enhanced red upconversion emission of Er3+-doped ZnO by post-annealing. Journal of Luminescence, 2017, 192, 668-674.	1.5	11
52	Localized surface plasmon resonance sensing structure based on gold nanohole array on beveled fiber edge. Nanotechnology, 2017, 28, 435504.	1.3	33
53	Modified FIR thermometry for surface temperature sensing by using high power laser. Optics Express, 2017, 25, 848.	1.7	16
54	Upconversion mechanisms of Er3+:NaYF4 and thermal effects induced by incident photon on the green luminescence. Journal of Luminescence. 2016, 175, 35-43.	1.5	25

#	Article	IF	CITATIONS
55	Effects of melting temperature and composition on spectroscopic properties of Er^3+-doped bismuth glasses. Optical Materials Express, 2016, 6, 279.	1.6	15
56	Concentration effects on the FIR technique for temperature sensing. Optical Materials, 2015, 43, 18-24.	1.7	23
57	Effects of alkali metal ions on upconversion photoluminescence intensity of Er3+-doped Y2O3 nanocrystals. Applied Physics B: Lasers and Optics, 2013, 110, 111-115.	1.1	21
58	Improved optical thermometry in Er3+:Y2O3 nanocrystals by re-calcination. Optics Communications, 2013, 309, 90-94.	1.0	19
59	Power dependence of upconversion luminescence of Er3+ doped Yttria nanocrystals and their bulk counterpart. Journal of Luminescence, 2013, 143, 423-431.	1.5	26
60	Suppression of energy transfer from Er3+ to OHâ^' in Er3+ highly doped zirconia. Optics Communications, 2013, 287, 228-233.	1.0	5
61	Effect of Li+ ions on enhancement of near-infrared upconversion emission in Y2O3:Tm3+/Yb3+ nanocrystals. Journal of Applied Physics, 2012, 112, .	1.1	47
62	Phase transformation of ZrO2 nanocrystals induced by Li+. Materials Letters, 2012, 79, 75-77.	1.3	10
63	Single band upconversion mechanisms of Er3+/Yb3+:ZrO2 nanocrystals. Optics Communications, 2012, 285, 1528-1532.	1.0	10
64	Optical temperature sensor through infrared excited blue upconversion emission in Tm3+/Yb3+ codoped Y2O3. Optics Communications, 2012, 285, 1925-1928.	1.0	140
65	Upconversion mechanisms and thermal effects of Er3+ in Er3+ doped yttria nanocrystals. Journal of Luminescence, 2012, 132, 1483-1488.	1.5	13
66	Efficient two-color luminescence of Er3+/Yb3+/Li+:ZrO2 nanocrystals. Optical Materials, 2011, 33, 1234-1238.	1.7	18
67	Optical thermometry through green and red upconversion emissions in Er3+/Yb3+/Li+:ZrO2 nanocrystals. Optics Communications, 2011, 284, 1876-1879.	1.0	48
68	Effects of Li+ on structure and spectroscopic properties of Er3+/Li+ codoped Sb2O3–Na2O–SiO2 glasses. Journal of Applied Physics, 2010, 107, 093103.	1.1	10
69	Intermacromolecular complexation due to specific interactions. 7. Miscibility and complexation between poly(styrene-co-4-vinyl benzoic acid) and poly[n-butyl methacrylate-co-(4-vinylpyridine)]. Journal of Macromolecular Science - Physics, 1998, 37, 827-839.	0.4	23
70	Intermacromolecular complexation due to specific interactions. 6. Miscibility and complexation between Poly{Styrene- <i>co</i> -[ <i>p</i> (2-Hydroxypropan-2-yl)Styrene]}and poly[ <i>n</i> -butyl Methacrylate- <i>co</i> -(4-vinylpyridine)]. Journal of Macromolecular Science - Physics, 1998, 37, 805-826.	0.4	22
71	Macromolecular aggregation: Complexation due to hydrogen bonding and hydrophobic association. Macromolecular Symposia, 1997, 124, 135-146.	0.4	7
72	Synthesis of monodisperse hydroxyl-containing polystyrene via chemical modification. Macromolecular Rapid Communications, 1996, 17, 37-42.	2.0	9